Report on a problem studied at the UK Mathematics-in-Medicine Study Group Southampton 2007
< http://www.maths-in-medicine.org/uk/2007/foot-and-mouth/ >

7TH MATHEMATICS IN MEDICINE STUDY GROUP

UNIVERSITY OF SOUTHAMPTON, 10–14 SEPTEMBER 2007

A simple mathematical model of the spread of Foot-and-Mouth Disease Virus through epithelial cells

John Ward (Loughborough University), Jennifer Thackham (Queensland University of Technology), Kel Heymer (University of Nottingham), Adriana Setchi (Imperial College London), Ebru Aydemir (University of Oxford), Zhidong Zhang, David Schley (Institute for Animal Health, Pirbright)

Abstract

Foot-and-mouth disease (FMD) is a significant socio-economic problem on a global scale. Furthermore, the disease causes considerable pain and suffering to the infected animals. The FMD virus is highly contagious and primarily infects epithelial cells in the tongue and feet regions, where resulting lesions can often develop.

The disease appears to behave quite differently in the epitheliums of the foot/tongue and the pharynx (soft palate). In the foot/tongue the virus tends to rapidly replicate, kill the host's epithelial cells, result in lesions and be cleared from the system. In the soft palate, however, the virus has been observed to replicate in a manner that is not fatal to the cells and persist for some time after the animal has recovered. There is considerable field evidence to indicate that these animals, while not exhibiting any outward signs of infection, may precipitate new outbreaks of disease. This clearly presents a problem to those who wish to prevent the spread of this disease.

The epithelial cells in the two regions are fundamentally the same, yet the virus behaviour is dramatically different. Here we will explore some of the potential mechanisms of the cell–virus dynamics that might be the cause of the different behaviour using mathematical modelling techniques. We are able to conclude that it may be the difference in epithelium thickness and susceptibility of the different layers of cells within the epithelium that is causing the observed differences of the virus in the palate and foot/tongue.

1 Introduction

Outbreaks have occurred in every livestock-containing region of the world with the exception of New Zealand, and the disease is currently enzootic (resident) in all continents except Australia and North America. The disease affects domestic cloven-hoofed animals, including cattle, swine, sheep, and goats, as well as more than 70 species of wild animals, including deer, The recent outbreaks of foot-and-mouth disease (FMD) in a number of FMD-free countries, in particular Taiwan in 1997 and the United Kingdom in 2001, have significantly increased public awareness of this highly infectious disease [3]. In 2001, the outbreak of Foot-and-Mouth Disease (FMD) cost the UK an estimated 8 billion: thousands of farmers lost their livelihoods, ten million sheep and cattle were killed to prevent the further spread of the disease and large areas of countryside were declared no-go zones thus decimating the domestic tourism industry. FMD is, therefore, of huge socio-economic importance and understanding its agent, FMD virus (FMDV), is vital in helping to control the spread of the disease.

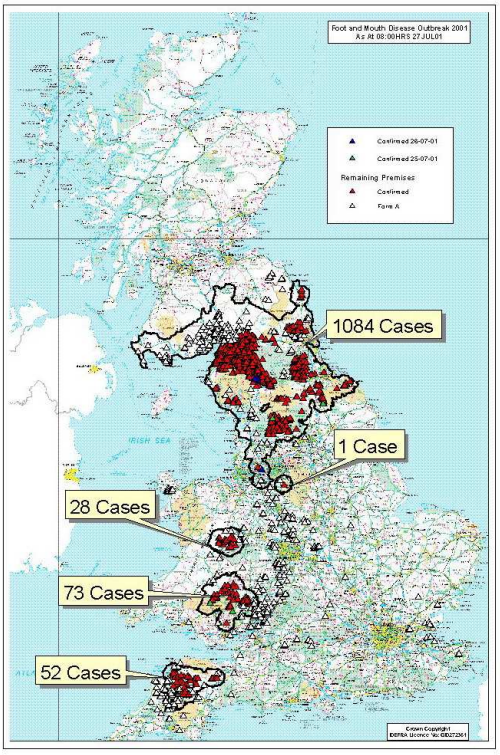

Figure 1: The confirmed cases of infected animals across the UK in 2001.

It has been reported that the virus attacks the epithelial cells in the foot/tongue region in a dramatically different way when compared to the soft palate, while the cells in each epithelium have fundamentally the same qualities [4]. We begin our investigation by summarising the

observed differences between the structure of the epithelium in the foot/tongue compared to the soft palate and also the different virus behaviours in the two regions.

1.1 Difference in Epithelium Structure

The target sites of FMDV replication are the epithelia from tongue, foot skin and pharyngeal region. The skin at these sites consists of a number of different cellular layers, which are illustrated in Figure 2. The stratum basale cells are involved in DNA synthesis and cell division and form a layer of around 1-2 cells thick. Some of the daughter cells of the stratum basale cells leave this cell cycle and differentiate into the spinosum, granulosum and corneum cells. As cells develop through the granulosum to the corneum, they die and become keratinised. The epithelia at the dorsal soft palate and the nasopharynx are highly specialized, non-cornified, stratified squamous epithelia, which are different from most of the surrounding epithelia. The special feature of this area is that the stratum corneum is absent and nuclei are retained in the terminally differentiating cells. These differences account for the thickness of epithelium in the foot/tongue region (about 230μm) being somewhat thicker than that of the soft palate (around 90μm). Furthermore, the proliferation rate of cells has been reported to be higher in the soft palate than in the foot/tongue.

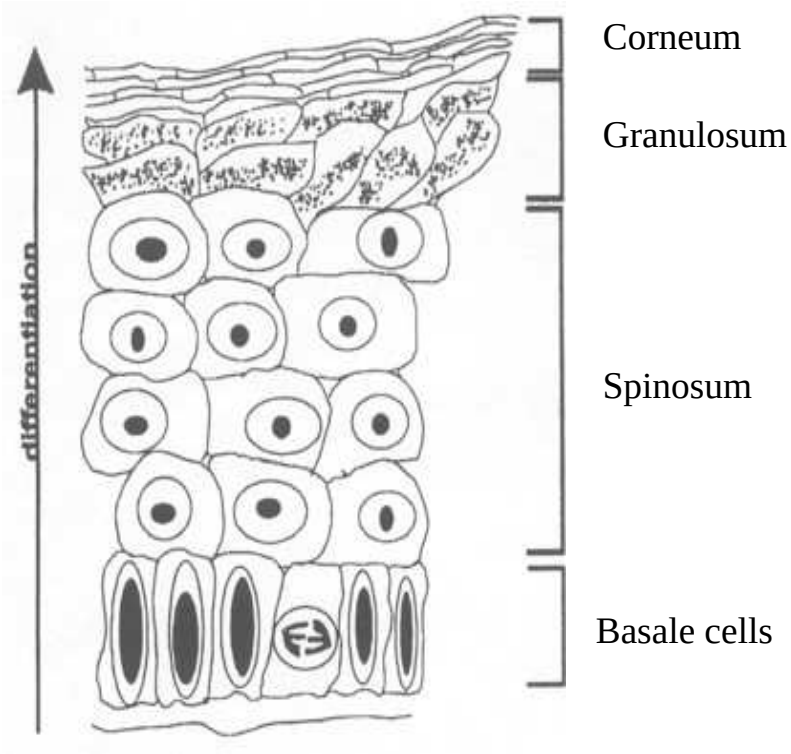

Figure 2: The different layers in the epithelium as would be found on the tongue and feet. In the palate the granulosum and corneum are absent.

1.2 Difference in Virus Behaviour

The virus appears to rapidly reproduce in the foot/tongue compared to the soft palate which explains the higher virus load that is commonly observed in the foot/tongue. This causes cell

death resulting in lesions on the tongue/feet. In the soft palate however, virus may persist at a low level without killing the host cells. Once the immune response has been initiated, the virus is cleared from the epithelium of the foot/tongue but tends to persist for much longer after the immune response has been initiated in the soft palate. Thus, animals that have no outwards signs of infection may still be able to contribute to the spread of the disease to other animals.

Table 1 summarises the differences in epithelium structure and virus behaviour in the two epithelium sites.

Epithelium of foot/tongue	Epithelium of soft palate
Thicker ($\sim$230μm)	Thinner ($\sim$90μm)
Top keratinised, cornified layer	No keratinised, cornified layer
Decreased proliferation	Increased proliferation
Lesions form	No lesions form
High level of viral load	Low level of viral load
Virus removed by immune system	Virus persists after infection

Table 1: Summary of the differences in structure and virus behaviour.

2 Hypotheses

Given the problem that we were presented with, it was our aim to use an appropriate mathematical model which might indicate which aspects of the epithelium are responsible for the different behaviour of the FMDV in the epithelium of the foot/tongue compared to the soft palate, with the hope that the results of the model might be able to help guide future experimental work. To achieve this aim, we began by establishing a hypothesis for the cause of the different virus behaviour.

2.1 Hypothesis One

Our first hypothesis was that it was an internal difference within the cells that was resulting in such altered virus behaviour. Based on this assumption, an intracellular mathematical model would seem appropriate. We hypothesised that this internal difference was causing a change in proliferation rate of cells in the two regions. However, further investigation of the literature revealed that there is no evidence of a *significant* difference in proliferation rates. We were subsequently required to modify our hypothesis.

2.2 Hypothesis Two

The second hypothesis that we established was that the difference in virus behaviour is due to two effects:

1. The thicker spinous layer in the foot/tongue compared to the soft palate epithelium.

2. The increased vulnerability of cells in the spinous layer to perish due to the virus.

We should note that, in what follows, the use of the terms basal and spinous cells may differ from the strict histological definition. For clarification, the use of these terms are meant in the following sense.

Basal cells: these are relatively young cells that are, by Hypothesis Two, assumed to have a greater level of resistance to viral presence. This may be due, for example, to the fact that the cells are sufficiently active and have sufficient nutrient supplies to compensate for any detrimental effect the virus may have. We expect the skin to have 3 or so cell layers that fall into this category.

Spinous cells: These are cells that have less resistance to the virus, perhaps due to being intrinsically less active or being deprived of sufficient nutrients to cope with exposure to viral particles.

3 Model Formulation

In order to develop a mathematical model of FMDV kinetics, we look to standard viral models to create a modelling framework to best describe the behaviour of the pathogen. We will focus on the early infection events prior to the active immune response, bout 4 days after contracting the virus.

As discussed previously, for this model we are only considering two types of cells that make up part of the epidermis, the basal and spinous cells. From the biology of the problem, we know that basal cells proliferate to create more basal cells and differentiate to spinous type. The production of basal cells is assumed to be logistic up to a maximum population carrying capacity. Although cells in the spinous layer can reproduce in the lower layers, we have made the simplifying assumption that in comparison to basal cells, the proliferation rate of spinous cells is negligible. Dependant on their bodily location, spinous cells can differentiate to form the keratinised layer or be sloughed off. Additionally, infected cells of both types can be removed from the system due to the virus causing lysis. That is, the host cells ruptures and releases newly created virus particles. These cell interactions are summarised diagrammatically in Figure 3.

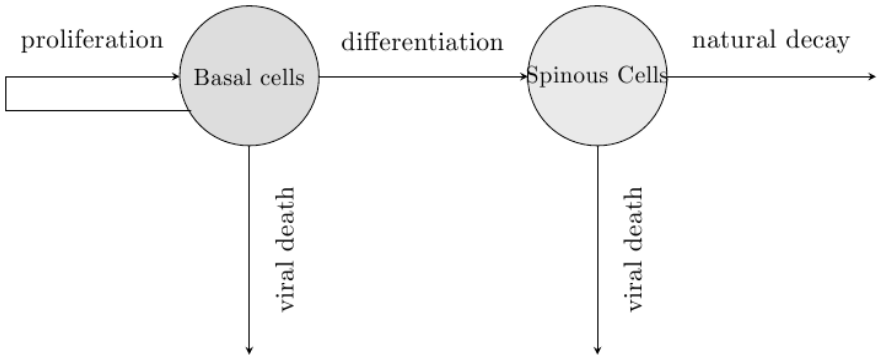

Figure 3: Schematic diagram illustrating the interactions between the basal and spinous cell populations.

In addition to considering the cells, we also need to consider the concentration of virus particles per unit volume within infected cells. Also, due to there being approximately 5% free

space within the epidermal extracellular-matrix (ECM), we also consider the concentration of virus particles extracellularly. For virus particles within basal cells, we consider two possible 'type' change events - to either spinous or extracellular. The virus particles within basal cells change to spinous type as the host cell differentiates or alternatively, change to extracellular virus as the particles are released when the host cell ruptures at lysis. Similarly, spinous virus can change to extracellular virus at lysis, or be removed from the system entirely when the spinous cell differentiates further or is sloughed off. Finally, extracellular virus can be removed from the system by being 'washed out' by the body, or change to basal or spinous virus by sucessfully infecting an unifected cell. These virus kinetics are summarised in Figure 4.

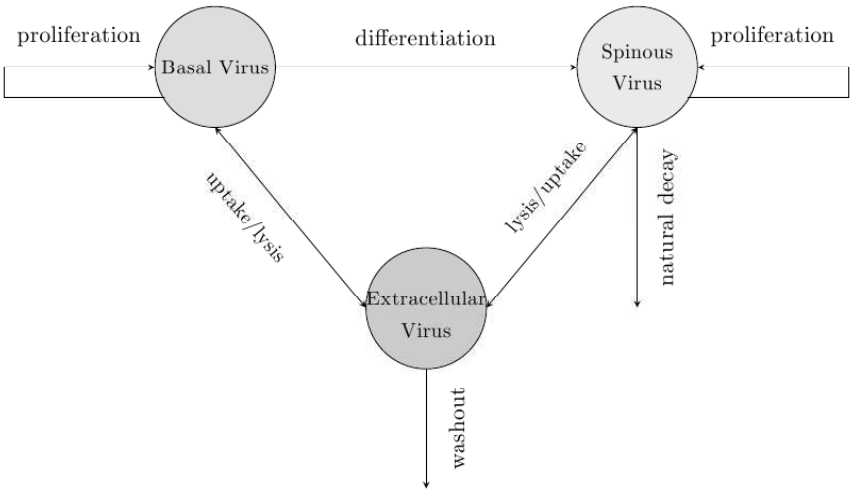

Figure 4: Schematic diagram illustrating the virus kinetics.

Once the key underlying processes of the virus behaviour have been identified, this allows us to form a mathematical model using ordinary differential equations (ODEs). The resultant system of ODEs will be discussed in Section 4.

4 The Governing Equations

Now that the important biological processes that must be considered for this model have been identified, we form our mathematical model using the technique of ODEs.

Our first system of ODEs have dimension, that is, each ODE describes the changes in cell population or virus concentration over time. We will denote B and S to be the (mean) number of layers of basal and spinous cells, respectively, and V_B, V_S, V_E to be the number of virus particles per basal cell volume in basal cells, spinous cells and extracellular fluid,

respectively. The equations are

$$\frac{dB}{dt} = rB(1-B/K) - \lambda B - \phi f_b(V_B)B \quad (1)$$

$$\frac{dS}{dt} = \lambda B - \gamma S - \phi f_s(V_S)S \quad (2)$$

$$\frac{d}{dt}(V_B B) = r_B V_B B(1-\frac{V_B}{V_K}) - \lambda V_B B - \phi f_b(V_B)V_B B + \mu V_E B \quad (3)$$

$$\frac{d}{dt}(V_S S\beta) = r_S \beta V_S S(1-\frac{V_S}{V_K}) + \lambda V_B B - \phi\beta f_s(V_S)V_S S + \alpha\mu V_E S - \beta\gamma V_S S \quad (4)$$

$$\frac{d}{dt}(V_E(N^*-B-\beta S)) = \phi f_b(V_B)V_B B + \beta\phi f_s(V_S)V_S S - \mu V_E(B+\alpha S) - \delta V_E(N^*-B-\beta S) \quad (5)$$

where

$$f_i = \frac{V_i^m}{V_{ic}^m + V_i^m} \quad (6)$$

is a "hill" function in V_i ($i = \{B, S\}$) that describes a substantial increase in cell death rate when the virus load exceeds a threshold density V_c.

Changes in the basal cell population are described by Equation (1). The first term is the logistic growth of basal cells at reproduction rate r, up to a maximum thickness governed by K and λ. The cell differentiation rate is denoted by λB and the final term describes the death rate of basal cells due to virus, according to the function $f_b(V_B)$. Similarly, for spinous cells in Equation (2) there is viral death, differentiation from basal cells and the second term which is a combined natural decay and differentiation (to keratinised layer) term, occurring at rate γ.

Equations (3 – 4) describe the evolution of the total virus numbers in the basal ($V_B B$) and spinous ($V_S S$) cell phases; the constant β is the average volume ratio between spinous and basal cells. Virus growth within cells is assumed to be limited (e.g. by availability of RNA and protein resources to generate new particles), and we model this behaviour using a logistic term. These equations also account for the differentiation of basal cells, particle loss through sloughing of material and the release of (following cell death) and internalisation of cells by viral particles. The constant α accounts for differences in propensity of the cell types to internalise viral particles from the ECM, e.g. due to differences in surface area and number of surface receptors. The evolution of extracellular virus particle density is described by equation (5) accounting for phase exchange and particles 'washed out' from the system into the surrounding media.

4.1 Parametrisation

The aim of the project is to investigate the different behaviour of the spread of FMDV in order to explain why the virus persists in the soft palate more than in the foot/tongue. Thus it is important to identify parameters in the mathematical model derived above that could potentially lead to a bifurcation between the two cases. Experimental work suggests that no significant changes are observed between the structure and function of individual cells from the soft palate and foot/tongue. Therefore, the parameters chosen to be investigated in the model will be ones that characterise the differences in layers in the epithelium.

Observations from image analysis (i.e. manually counting cells from a photograph of skin slices viewed under a light microscope) suggest that the number of living cell layers in a healthy soft palate is around 9 and there are about 20 layers in the skin of the foot and tongue. It is expected that, on the basis of informed opinion, that the number of basal cells would consist of about 3 layers in both cases, hence the virus-free steady-state values (B^*, S^*) can be taken to be

$$B^* = 3, \qquad S^* = \begin{cases} 6 & \text{in soft palate} \\ 17 & \text{in foot/tongue} \end{cases}$$

There is a significant difference between the ratio B^*/S^* for the soft palate and foot/tongue scenarios that will be studied with regards to the investigation of Hypothesis Two. It should be stressed that the quoted numbers are taken to be the approximate mean number of cell layers across a skin surface of many millions of cells. These values of B^* and S^* will form the initial conditions at the time when virus is introduced to the system.

Using (B^*, S^*) as a basis, we make the following assumptions on some of the parameters

$$N^* = \frac{B^* + \beta^{1/3} S^*}{1-w}, \qquad K = \frac{B^*}{1-\lambda/r}, \qquad \frac{\gamma}{\lambda} = \frac{B^*}{S^*}.$$

Here the maximum number of cells with single basal cell thickness, N^*, is calculated with the assumption that there is a constant void fraction w (typically $w \approx 0.05$) throughout. We note the $\beta^{1/3}$ resulting from an edge length of an assumed cuboidal spinous cell. The second and third terms come from the steady-states of (1) and (2) in the absence of virus.

We can make a very crude estimate of the order of magnitude of the ratio δ/μ based on distances of the whole skin domain and average distances between cells in healthy skin, assuming a high virus affinity to cell membranes and/or receptors. Let l be the side length of a basal cell, then the skin thickness will be $N^* l$, of which the total gap length will be $wN^* l$, thereby the average gap length is $wN^* l/(B^* + S^*)$. Assuming that δ and μ are inversely proportional to the distance needed for the virus particles to travel the thickness of the skin and across gaps between cells, respectively, then

$$\frac{\delta}{\mu} = \frac{w}{B^* + S^*}. \tag{7}$$

Typical parameter values suggest that δ/μ is likely to be small, which implies that there is a fairly low level of virus escape from the system.

The values for r_S and r_B are based on published data [2]. The values for V_{Bc} and V_{Sc} are chosen to yield the best shape for the Hill functions used to model the virus spreading. Experimental data suggests that three hours is the longest period of time it takes for the virus to infect a maximum of cells in the domain [1]. Thus ϕ is taken to be 1/3.

Therefore, we have derived a system of differential equations with consistent initial conditions and have found or approximated all parameters in the system. Thus the problem can now be analysed analytically and numerically. Next, we look at the nondimensionalisation of the system.

4.2 Non-dimensionalisation

We non-dimensionalise the system using the rescalings

$$t = \frac{\hat{t}}{\lambda}, \quad B = K\hat{B}, \quad S = K\hat{S}, \quad V_B = V_K \hat{V}_B, \quad V_S = V_K \hat{V}_S, \quad V_E = V_K \hat{V}_E,$$

	Soft Palate	**Foot/Tongue**
Non-trivial steady state for the number of basal cells in the absence of virus B^*	3	3
Non-trivial steady state for the number of spinous cells in the absence of virus S^*	6	17
Differentiation rate of basal cells λ	$1/96$ hr^{-1}	$1/96$ hr^{-1}
Reproductive rate of basal cells r	$1/24$ hr^{-1}	$1/24$ hr^{-1}
Virus replication rate in basal cells r_B	18 hr^{-1}	18 hr^{-1}
Virus replication rate in spinous cells r_S	18 hr^{-1}	18 hr^{-1}
Maximum rate at which virus kills cells ϕ	$1/3$ hr^{-1}	$1/3$ hr^{-1}
Virus threshold value in basal cells V_{Bc}	2×10^4	2×10^4
Virus threshold value in spinous cells V_{Sc}	2×10^4	2×10^4
Carrying capacity of basal cells K	4	4
Carrying capacity of virus in cell K_v	2×10^5	2×10^5

Table 2: Estimated parameter values in the soft palate and the foot/tongue.

where the characteristic timescale of the problem is taken to be based on the differentiation rate λ^{-1} of approximately 4-5 days and V_k represents a characteristic viral concentration. We also define

$$\hat{r} = \frac{r}{\lambda}, \ \hat{\phi} = \frac{\phi}{\lambda}, \ \hat{\gamma} = \frac{\gamma}{\lambda}, \ \hat{r}_B = \frac{r_B}{\lambda}, \ \hat{r}_S = \frac{r_S}{\lambda}, \ \hat{\mu} = \frac{\mu}{\lambda}, \ \hat{\delta} = \frac{\delta}{\lambda},$$
$$\hat{V}_{Bc} = \frac{V_{Bc}}{V_K}, \ \hat{V}_{Sc} = \frac{V_{Sc}}{V_K}.$$

Dropping the hats on the dimensionless terms, as is customary, we get

$$\frac{dB}{dt} = rB(1-B) - B - \phi f_b(V_B)B \tag{8}$$
$$\frac{dS}{dt} = B - \gamma S - \phi f_s(V_S)S \tag{9}$$
$$\frac{d}{dt}(V_B B) = r_B V_B B(1-V_B) - V_B B - \phi f_b(V_B)V_B B + \mu V_E B \tag{10}$$
$$\frac{d}{dt}(V_S S\beta) = r_S \beta V_S S(1-V_S) + V_B B - \phi\beta f_s(V_S)V_S S + \alpha\mu V_E S - \beta\gamma V_S S \tag{11}$$
$$\frac{d}{dt}(V_E(N^*-B-\beta S)) = \phi f_b(V_B)V_B B + \beta\phi f_s(V_S)V_S S - \mu V_E(B+\alpha S) - \delta V_E(N^*-B-\beta S) \tag{12}$$

Viral events in the ECM (e.g. attachment to skin cell, dispersal in and washout from the skin structure) are likely to occur very rapidly in comparison to the timescale of interest and we will assume that V_E is quasi-steady, hence

$$\mu V_E = \frac{\phi(f_b(V_B)V_B B + \beta f_S(V_S)V_S S)}{B + \alpha S + \frac{\delta}{\mu}(N^* - B - \beta S)}, \tag{13}$$

which can be substituted into Equations (8)-(11), reducing our system from 5 to 4 equations.

The δ/μ ratio (7) then becomes

$$\frac{\delta}{\mu} = \frac{w}{K(B^* + S^*)}.$$

5 Steady-state analysis

5.1 Analysis of the viral-free case

Imposing $V_B \equiv 0$ and $V_S \equiv 0$ on Equations (8) and (9) results with the reduced system

$$\frac{dB}{dt} = rB(1-B) - B, \tag{14}$$

$$\frac{dS}{dt} = B - \gamma S, \tag{15}$$

which describe the healthy skin state. It is straightforward to show that the steady-states (B^*, S^*) are

$$(B^*, S^*) = (0,0), \quad \left(\frac{r-1}{r}, \frac{r-1}{\gamma r}\right)$$

from which physicality of the non trivial solution implies $r > 1$. It can be shown that this steady state is linearly stable given this constraint. For $r > 1$, the trivial solution is linearly unstable, thus the model predicts full recovery following a viral infection.

5.2 Analysis of the full system

The equivalent analysis on Equations (8) - (11) and Equation (13) is more of a challenge and the types of solutions are summarised below; we note the analysis here is not yet complete. It is understood that the vectors denoted in the table and the cases below are ordered thus (B, S, V_B, V_S).

	$0 < r < 1$	$1 < r < 1 + \phi f_b(\overline{V_B})$	$1 + \phi f_b(\overline{V_B}) < r$
$\frac{r_S}{\gamma} > 1$ $r_B > 1$	$(0,0,V_B^0,V_S^0)$ S	$(0,0,V_B^0,V_S^0)$ CS $(B^*,S^*,0,0)$ U	$(0,0,V_B^0,V_S^0)$ U $(B^*,S^*,0,0)$ U $(\overline{B},\overline{S},\overline{V_B},\overline{V_S})$ S? N?
$0 < \frac{r_S}{\gamma} < 1$ $0 < r_B < 1$	$(0,0,V_B^0,V_S^0)$ S	$(0,0,V_B^0,V_S^0)$ CS $(B^*,S^*,0,0)$ S	$(0,0,V_B^0,V_S^0)$ U $(B^*,S^*,0,0)$ S $(\overline{B},\overline{S},\overline{V_B},\overline{V_S})$ E? N?

Table 3: A "very much in development" table summarising the linear stability of the main classes of steady-state solutions in the key parameter regimes. Here the notation 'S', 'U', and 'CS' refers to a stable, unstable or conditionally stable steady state, respectively. Furthermore, 'E' refers to the existence of a steady state and 'N' to the number of steady states that may or may not exist.

- $\underline{E^V = (0, 0, V_B^0, V_S^0)}$: This is a family of solutions, whereby all positive real values of V_B^0 and V_S^0 are valid steady states. The linear stability is conditional on the value of V_B^0 in that E^V is stable if and only if $r < 1 + \phi f_b(V_B^0)$. This family represents the case when there are no cells left and thus the total number of virus in the system is zero. The actual values of V_B^0 and V_S^0 at the steady-state will be dependent on the initial conditions.

- $\underline{E^* = (B^*, S^*, 0, 0) = (1 - \frac{1}{r}, \frac{1-\frac{1}{r}}{\gamma}, 0, 0)}$: This steady state represents full skin recovery, where it is assumed, from the analysis in the viral-free case, that $r > 1$. Moreover, it can be shown that E^* is linearly stable if and only if $r > 1$ and $r_B < 1$ and $r_S < \gamma$, representing weak viral growth in the basal cells (at a rate slower than basal cell growth) and spinous cells (growth rate is less than spinous differentiation/loss rate).

  The data values suggest that this scenario is very unlikely.

- $\underline{\overline{E} = (\overline{B}, \overline{S}, \overline{V_B}, \overline{V_S})}$: This steady state represents a coexistence state of cells and virus. The analysis for this case is difficult and could not be completed within the time frame of the Study Group. Furthermore, it is not clear whether there are one or more such solutions given a parameter set. However, there is an existence condition, namely $r > 1 + \phi f_b(\overline{V_B})$, whereby one solution is very likely to be linearly stable when $r_B > 1$ or $r_S/\gamma > 1$. Numerical solutions support this notion. A complete analysis of this case will be undertaken in due course.

Table 3 shows a summary of the results obtained, indicating points of bifurcation between the various steady-state types in terms of the parameters r, r_B and r_S/γ. It also suggests that there has to exist at least one non-trivial steady state that is stable when $1 + \phi f_b(\overline{V_B}) < r$ and $r_S/\gamma > 1$ and $r_B > 1$ as the other states are unstable. It is this region that contains the case described by the parameter values chosen in the previous section. The stable steady state found numerically supports these findings.

6 Numerical simulations

The non-dimensional system of ODEs (8)-(11) and Equation (13) was solved using a backward difference solver, implemented in the Numerical Algorithms Group (NAG) routine D02EJF. Due to the immune system becoming effective from about four days (dimensionless time $t \approx 1$) after the initial viral insult, which the current model does not account for, all simulations are run up to $t = 1$. In all the simulations discussed below the system was seeded with a small amount of virus ($V_B = 0.001$ and $V_S = 0.001$) at $t = 0$.

The dimensionless versions of the values, shown in columns 2 and 3 of Table 4, did not produce results consistent with experimental observations so, given that these number where obtained somewhat crudely, it gave us some license to adjust them. The modified values are shown in columns 4 and 5 of Table 4. The main adjustment is the increase from 3 to 6 basal cells (so adjusting parameter K from 4 to 8). Other adjustments include the moderate reduction in ϕ (reducing viral potency) and the somewhat more substantial reduction in r_B and r_S (reducing virus particle replication rate). The experimental data for these values will be in conditions that are optimum for virus effects, so reduced values of these parameters is justifiable. In accordance with Hypothesis Two, we assume that basal cells have greater resistance against the virus than spinous cells, and we choose the hill function parameter to

reflect this, namely $V_{Bc} = 2 > V_{Sc} = 0.8$. It should be stressed that the values are chosen to demonstrate that the model can reproduce qualitatively the skin's observed response to a virus challenge.

6.1 Results

Figure 5 shows the response of basal cells (solid line) and spinous cells (dashed line) to a virus insult. In the foot/tongue scenario (Figure 5(a)), there appears to be an initial period in which there are little observable effects for the first 12 hours or so (recall $t \approx 0.25$ represents 1 day), corresponding to a relatively low virus load (see Figure 7(b)). Over this period, the virus multiplies within the cells and as we can see from Figure 5(a) the spinous cells in particular begin to die off sharply (which would result in the observed lesions). The enhanced resistance of the basal cells ensures the virus has relatively little effect on these cells.

There is a qualitatively similar, but less well marked, predicted outcome for the palate case (Figure 5(b)). Whilst the basal cells are relatively unharmed, the spinous cell thickness has reduced to about a third of the original thickness (as opposed to about 10% in the foot/tongue scenario).

Figure (6) shows the viral load in each of the cell types and extracellular fluid in both scenarios. The profiles of the internal virus are similar in both these scenarios, with the only significant difference being the higher extracellular virus load in the foot/tongue case from days 1-3. This is due to the combined effects of increased cell death leading to greater particle release and the smaller ratio δ/μ reflecting a thicker skin which allows for a greater accumulation of the particles. However, by day 4 the virus loads are decreasing and will converge due to the skin structure being more or less the same in both scenarios (Figure 7(a)).

	Dimensionless values		Values used in simulations	
Parameter	**Foot/Tongue**	**Soft Palate**	**Foot/Tongue**	**Soft Palate**
B^*	0.75		0.75	
S^*	4.25	1.5	1.75	0.375
r	4		4	
ϕ	32		8	
$\gamma = B^*/S^*$	0.12	0.5	0.429	2
r_B	1728		20	
r_S	1728		20	
$\delta/\mu = w/K(B^* + W^*)$	0.0025	0.0056	0.0025	0.0056
α	-		1	
β	-		1	
V_{Bc}	0.1	0.1	0.8	2
V_{Sc}	0.1	0.1	0.8	2
m	-		2	

Table 4: Calculated dimensionless parameter values based on values in Table 2 and parameter values used in simulations. For the simulations the dimensional value of B^* is taken to be 6, which resulted with the value of the "carrying capacity" $K = B^*/(1 - 1/r)$ changing from 4 to 8.

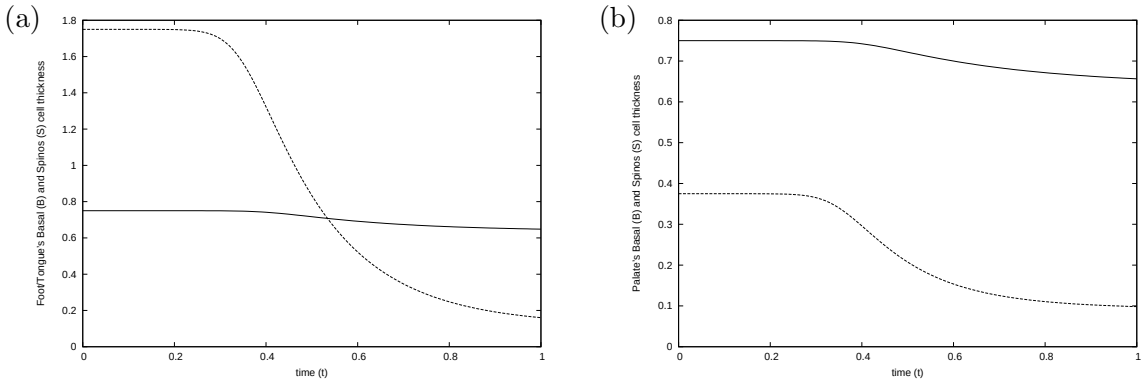

Figure 5: Plots of the skin cell type's response to an introduced virus over the first 4 days ($t = 1$) in the foot/tongue (a) and palate (b). Here the dashed curve represents the spinous cell population while the solid line corresponds to the basal cells.

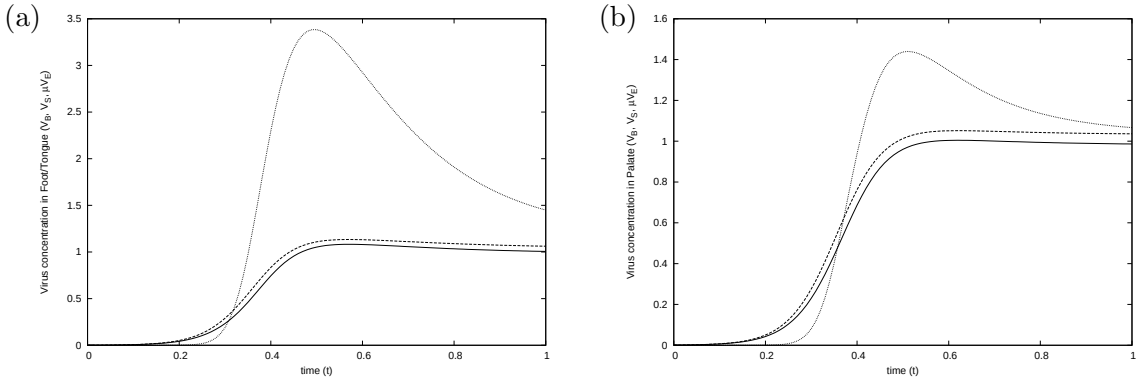

Figure 6: Plots of the evolution of the viral load in basal cells (solid), spinous cells (dashed) and extracellular fluid (dotted) in the skin of the foot/tongue (a) and palate (b) over the first 4 days.

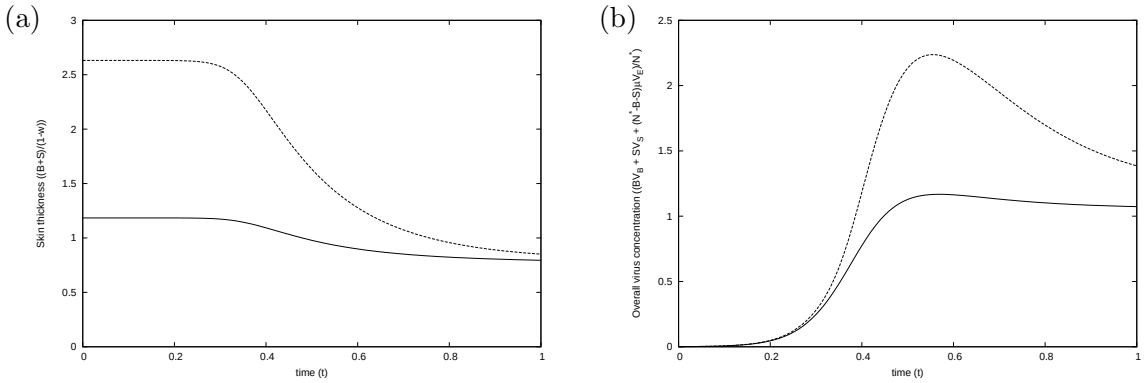

Figure 7: Plots of the evolution of skin thickness (a) and total virus load (b) over the first 4 days. Here the dashed curve represents the foot/tongue epithelium while the solid line corresponds to the palate.

The total skin thickness $(B + S)/(1 - w)$ is shown in Figure 7(a), in which the palate and foot/tongue responses are indicated by the solid and dashed curves, respectively. As indicated above, the skin thickness of the foot and tongue reduces substantially, whereas the palate cells

only slightly, over the course of the 4 days. Interestingly, this simulation predicts that the resulting thicknesses are approximately the same. However, in practice, the wear and tear the skin experiences varies between the different sites, whereby in the palate, presumably where there is less wear and the skin integrity is maintainable, but not so in the foot and tongue.

In the foot/tongue scenario, the overall virus concentration ($(V_B B + V_S S + \mu V_E(N^* - B - S))/N^*$) is shown to peak after about 2 days (Figure 7(b)) before slowly trailing off. This is consistent with observations of animals infected by the virus. The trailing off is due to there being fewer cells remaining to harbour the virus for growth. In contrast, in the palate, the overall virus concentration rises towards an upper level which is approximately maintained. This prediction should be investigable from examination of the virus in the palate skin layers.

7 Conclusions and Future Work

This report describes an initial attempt at investigating the reasons why there are significant differences between FMDV action on skin cells in the foot and tongue areas and epithelial cells in the soft palate. With there being no apparent differences between the cells at these sites, a hypothesis (Hypothesis Two) was proposed based on the histological differences in epithelial structure between the foot/tongue and palate. In particular it was proposed that the palate consists of a greater proportion of basal cell layers (though the locations have the same number of these layers, i.e B^* is fixed in both cases), which are hypothesised to be more resistant to the presence of the virus (i.e. $V_{Bc} > V_{Sc}$). The system of ODEs derived were based on biologically realistic assumptions. Numerous simplifying assumptions were made in order to construct a model that was able to be analysed within the time frame of the Study Group. Most notably the model neglects spacial considerations. Despite this, the resulting model has many of the seemingly important features and existing experimental work has enabled some level of parameter estimation. Some adjustment was made to the originally proposed parameters in order to obtain results with the appropriate qualitative behaviour, but the significant changes (i.e. over orders of magnitude) were only made to the virus growth rate parameters V_B, V_S, r_B and r_S.

The numerical simulations do demonstrate that differences in skin structure in the foot/ tongue and palate scenarios can generate results that broadly agree with experimental observations. We can only be tentative with our conclusions at this stage, but, at the very least, the model suggests that the mechanisms proposed in Hypothesis Two do form a plausible explanation for the observed differences. Some predictions from the modelling that perhaps have not been considered, observed or measured previously in experiments include:

- In the first 4 days, virus loads within cells in all layers of the skin are about the same in both scenarios.
- The total virus load in the palate remains approximately constant after a few days of infection.
- The number of layers of living cells in the foot/tongue and palate are approximately the same following a few days of infection.

There is considerable scope for further work. As yet the steady-state analysis is incomplete. There are many aspects believed to be important, which are lacking in the current model, such

as pH levels, temperature, keratinisation and the immune response. Spatio-temporal variations are likely to be important and expansion of an infection from a very localised infection would be interesting. Directly applicable experimental data was found to be limited and a number of guesses and approximations were needed to compile Table 4: clearly, further work is needed in the area acquiring suitable and accurate data. More accurate modelling should offer new insights into the infection processes of the FMDV and could open up possibilities for improved or novel procedures for the management of the disease.

References

[1] F. Cartwright *et al.* (1957). *J. Gen. Microbiol.*, **16**, 730–748.

[2] B.N. Fields *et al.* (1996). *Picornaviridae:* the viruses and their replication. In Fields Virology (3rd Ed.), Ed. B.N. Fields *et al.*. Lippincott-Raven, USA.

[3] M.J. Grubman and B. Baxt (2004). *Clin. Microbiol. Rev.*, **17**, 465–493.

[4] Z. Zhang and S. Alexandersen (2004). *J. Gen. Virol.*, **85**, 2567–2575.